Tailoring the Polymeric Nanoparticles for Rubber Reinforcement

Chenchy J. Lin, Xiaorong Wang

Bridgestone Americas Center for Research and Technology, Akron, Ohio 44317

Received 4 January 2010; accepted 9 May 2010
DOI 10.1002/app.32762
Published online 27 July 2010 in Wiley Online Library (wileyonlinelibrary.com).

ABSTRACT: Polymeric nanoparticles with brush-like polydiene as the shell and crosslinked polystyrene as the core are synthesized using anionic polymerization via a self-assembly process of macromolecules in solutions. The microstructures of nanoparticles were designed to match those of the matrix polymer used for tire compounds. Desirable compound properties were obtained by tailoring the shell sizes of the nanoparticles. Depending on the core/shell structures of the nanopartilces, the addition of the nanosized particles may impart the compound ultimate physical properties. Well reinforced compounds with enhanced dynamical storage modulus (G') without increasing their dependences on temperature and deformation strain can be obtained by the addition of the nanoparticle with lengthened shell chains. Improved tensile mechanical properties without increasing high-temperature hysteresis were also attained by such reinforcement. Passenger and truck tire applications can be advantageously benefited from these properties with improved tire handling and cornering consistence without increasing the rolling resistance and the sacrifices of other performances. A miscibility study was conducted on various binary blends of nanoparticle and rubber matrix. The compatibility between the nanoparticle and the matrix rubber along with the core concentration were demonstrated to be responsible for the observed improved compound properties. © 2010 Wiley Periodicals, Inc. J Appl Polym Sci 119: 768–775, 2011

Key words: nanoparticle; core and shell; rubber; reinforcement

INTRODUCTION

Automotive industry has been increasingly demanded better driving performances from tire contributions, including crisper handling, better steering stability, and lower rolling resistance. The stiffness of a rubber tread is generally associated with its handling performance. Increasing tread dynamic stiffness will improve the tire handling performance by decreasing the tread block deformation in aggressive driving courses.[1] A tread rubber with high hysteresis loss upon deformation will usually give good road traction grips.[2] However, the higher traction by means of increasing hysteresis loss upon deformation is adversely undesirable because it increases the tire rolling resistance. In addition, significant heat will build up to increase the tire temperature during continuous high-speed running. Tire handling and steering stabilities will deteriorate due to the decreased dynamic storage modulus (G') as the temperature increases. Therefore, it remains a great deal of challenge for scientists and engineers to attain a tire tread having improved tire handling, corning, and driving consistence without increasing its rolling resistance.

Rubbers stiffness can be enhanced by simply loading more filler or by increasing crosslinking level therein. However, these two approaches will lead to unsatisfactory results such as high hysteresis, poor aging properties, and poor wear resistance. Other methods with the inclusion of polyolefin were reported.[3–8] However, there are some shortcomings associated with these approaches. For example, the high temperature dependence of the compounds containing polyolefin has limited them to nontread application only. To addresses this issue, an approach of using core/shell type polymeric nanoparticles to enhance the rubber compound G' and mechanical properties was reported in this article.

Core/shell type polymeric nanoparticles had been used for various tire compound applications.[9–13] However, tire compound properties with inclusion of the nanoparticles strongly depend upon the particle structures. Desired compound properties with these polymeric particles can only be attained through the use of an appropriately designed structure in particle. In this work, we show that tire rubber compounds can be advantageously modified by addition of the nano-sized polymeric particles with special designed core/shell structures. Mechanical properties of a rubber compound are enhanced by inclusion of the nano-sized cores, whereas the

Correspondence to: C. J. Lin (linjeffrey@BFUSA.com).

TABLE I
Characterization Data of the Polymeric SBR-PS Nanoparticles

	Duradene™ SBR	SBR-PS-1	SBR-PS-2	SBR-PS-3
M_w of SBR[a], g/mole	350,000[b]	53,900	102,400	115,720
M_w of single PS chain in micelle hard core	N/A	25,000	25,000	25,000
Volume % of nano particles	N/A	27	16	14
Polydispersity[c]	1.1–1.8	1.09	1.12	1.10
% Styrene[d]	23.5	60.6	46.5	42.4
% Vinyl[d]	47	19.4	26.8	22.5
T_g °C[e]	−36	−36 and 65	−35 and 74	−45 and 86
Mean Size of Nanoparticle (nm)[f]	N/A	44	47	52

[a]Based on the M_w of the brush and hard-core particle.
[b]Provided by Firestone Polymers LLC for synthetic rubber.
[c]By GPC measurement.
[d]By 1H-NMR.
[e]By DSC.
[f]By TEM.

compatibility issue between the hard cores and the matrix is addressed through the penetration of the shell into the rubber matrix. More specifically, use of tailored nanoparticles in rubber compounds was demonstrated to enhance G' without increasing the G' temperature and strain dependences. Favorable and consistent tire performances such as wet traction, rolling resistance, and handling properties are also attained from these compounds containing such particles.

EXPERIMENTAL

Preparation and characterization of polymeric nanoparticles

Synthesis process[10,12]

Polymeric nanoparticles of PS-SBR with core–shell structures were prepared by anionic polymerization in hexane solution of 12 wt % of diene monomers through three stages. In the first stage, butadiene (BD) and styrene (ST) were charged into a reactor, the polymerization was initiated with butyl lithium (BuLi) and the microstructure was controlled by adding oligomeric oxolanyl propane polar randomizer. The polymer molecular weight (M_w) was controlled by adjusting the ratio of the monomers and level of initiator used. After nearly all of the monomers were consumed in the first stage, additional ST was charged for polymerization to form the micelle core in the second stage. The M_w of PS in the core was adjusted to be about 25,000. Then, 8 wt % of divinyl benzene relative to the particles was then charged into the reactor in the third stage to cross-link the micelle core. The polymerization temperature was maintained at about 57°C throughout the polymerization. The final material was isolated by adding a mixture of acetone and isopropanol in a volume ratio of 95% to 5%. *t*-Butyl-2-hydroxy toluene was then added into the polymer as an antioxidant. The characterization of these nanoparticles including M_w, the particle size, polydispersity, polymer microstructure, and T_g are tabulated in Table I.

Characterization

The nanoparticles were characterized by the transmission electric microscopy (TEM), NMR, thermal analysis, and gel permeation chromatography (GPC) measurements. Detailed descriptions on the formation of shell–core structure of nanoparticles had been discussed in a prior publication.[12]

Transmission electric microscopy

The sizes of nanoparticles were characterized by the TEM. In preparation, about 10 mL of solution was taken from the polymerization batch and further diluted with the hexane solvent to about 10^{-4} wt %. A drop of the diluted solution was then deposited on a formvar-carbon coated microgrid. After the solvent was evaporated, the grid was stained with OsO_4, and then examined by TEM. The results shown in Figure 1 indicates that the average particle diameter was about 50 nm dispersed relatively uniform with polydispersity of about 1.1.

^{1}H-NMR measurements

The polymer microstructure such as vinyl and ST content were determined by the ^{1}H-NMR measurements. A Varian Gemini 300 NMR Spectrometer System was used. Polymer were dissolved in a deuterated solvent ($CDCl_3$) and filtered before being transferred into a NMR tube for measurement.

Thermal analysis

Thermal analysis was performed on a TA instruments DSC 2910 using a nitrogen-purged cell at a flow rate of 80 mL/min. The DSC cell was calibrated

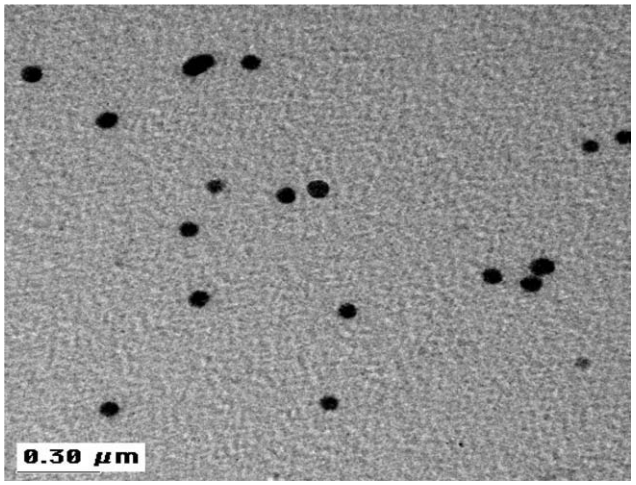

Figure 1 The TEM micrograph of the polymeric SBR-PS nanoparticle.

with Indium at 10°C/min heating rate. T_g was determined as the temperature where an inflection point of the heat capacity (C_p) change.

GPC measurement

GPC measurements were carried out on a Waters Model 150-C instrument with tetrahydrofuran (THF) as the solvent. Solid samples were weighed, dissolved in THF, and filtered before injection into the GPC columns. The columns were calibrated using polystyrene standards, and the averaged molecular weight of the sample was estimated based on these standards and a universal calibration curve.

Rubber compounding and evaluation methodologies

Preparation of rubber compounds

The formulations used for preparing rubber compounds for this study are shown in Tables II. The

TABLE II
Formulations Used for Preparing the Rubbers for this Study

Ingredient	phr
SBR	Varied
SBR-PS micelle Polymer	Varied
Carbon black	Varied
Process oil (Aromatic oil)	10
Wax	1.0
Antioxidant [*N*-(1,3 dimethylbutyl)-*N*′-phenyl-*p*-phenylene-diamine]	0.95
Stearic acid	2.0
Sulfur	1.3
Accelerator [*N*-Cyclohexyl-2-benzothiazolesulfenamine](CBS)	1.7
Zinc oxide	2.5
Diphenyl guanidine (DPG)	0.2
Zinc Oxide	2.5

TABLE III
The Mixing Procedures Used for Preparing Rubber Stocks

Mater batch stage (MB)	310 g Brabender
Agitation speed	60 rpm
Initial temperature	100°C
Mixing at 0 s	Charging polymers and micelle polymers (if added)
Mixing at 30 s	Charging fillerprocess oil, wax, antioxidant, and stearic acid.
Target drop temperature	170°C
Remill 1 (R1) batch stage	
Agitation speed	60 rpm
Initial temperature	70°C
Mixing at 0 s	Charging MB stock
Target drop temperature	145°C
Final batch stage	
Agitation speed	45 rpm
Initiation temperature	90°C
Mixing at 0 s	Charging remilled stock
Mixing at 30 s	Charging the curatives
Target drop temperature	104°C

DURADENE™ poly(butadiene-*co*-styrene) polymer (SBR) was obtained from Firestone Polymers, LLC[1*] The amounts of the ingredients used are normally given based on a total of 100 parts of the rubber or combination of rubbers used. Four stocks of rubbers were prepared using the formulation and mixing conditions shown in Tables II–IV. One hundred phr of SBR DURADENE™ SBR was used to prepare Stock 1, the control stock. In Stocks 2–4, 10 phr of DURADENE™ SBR was replaced with polymeric nanoparticles of various shell sizes and the compositions are shown Table IV. The final stocks were sheeted and then subsequently molded at 171°C for 15 min.

Evaluation methodologies

Dynamic mechanical viscoelastic property measurements

The dynamic viscoelastic properties of cured stocks were obtained from temperature and strain sweep experiments using Rheometrics Dynamic Analyzer models RDA-700 and RDA-II. Rheological data such as storage modulus (G') and loss modulus (G''), strain, shear rate, viscosity, and torque were measured. Temperature sweep experiments were conducted with a frequency of 5 Hz using 0.5% strain for temperature ranging from −100 to −10°C, and 2% strain for the temperature ranging from −10 to 100°C. Test specimens used for dynamic temperature sweep test are rectangular slabs with dimensions of 27 mm × 12.5 mm × 2 mm in length, width, and thickness,

*Duradene is a registered trademark of Firestone Polymers LLC for synthetic rubber.

TABLE IV
SBR and SBR-PS Used to Prepare Stocks 1 to 4

Stock No.	SBR	SBR-PS-1	SBR-PS-2	SBR-PS-3
1	100	0	0	0
2	90	10	0	0
3	90	0	10	0
4	90	0	0	10

respectively. A frequency of 0.5 Hz was used for strain sweep with strain sweeping from 0.25 to 14.75%. The sample geometry used for strain sweep test is cylindrical with 9.5 mm in diameter and 15.6 mm in length. Payne effect ($\Delta G'$) and tan δ at 5% strain were obtained from the strain sweep experiment.

Mechanical properties assessments—Tensile mechanical properties

The tensile mechanical properties were measured using the standard procedure described in the ASTM-D-412[14] at 25°C. The tensile test specimens are dumbbell shape with a dimension following the ASTM-D-412 dumbbell die but 0.19 cm in thickness.

RESULTS AND DISCUSSIONS

The G' temperature and strain dependences of Stocks 1–4 are shown in Figures 2 and 3, respectively. Increased G' (20–53%) was found in rubber compounds containing polymeric nanoparticles SBR-PS over the measured temperature and strain ranges shown in Figures 2 and 3. The G'increases in these stocks are attributed to an enhanced hydrodynamic effect[15–17] imparted by the presence of the additional hard domains donated by the core parts of the nanoparticles. Higher degree of G' enhancement was found in stocks containing nanoparticles with shorter shell lengths due to the presence of more hard core domains when compared with those with longer shells. Note that the core volume fractions of the nanoparticles SBR-PS-1, SBR-PS-2, and SBR-PS-3

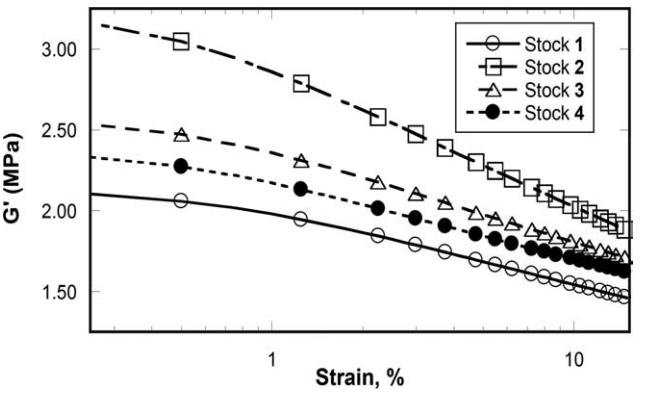

Figure 3 The G' strain dependences of Stocks 1–4.

are 27%, 16%, and 14%, respectively. Therefore, it is not surprising to find the G' enhancement in the order of Stock 2 > Stock 3 > Stock 4 > Stock 1 at a given nanoparticle loading in these compounds. Increasing tread dynamic stiffness will improve the tire handling performance due to less tread block deformation in aggressive driving. Therefore, it is of desire to have these rubber compounds with increased G' as the tire tread to improve the tire handling performance. However, with more hard core presences in Stock 2, stronger G' temperature and strain dependences were also found when compared with others. (See Figs. 2 and 3). This will increase the handling sensitivity during the driving courses which is not desirable for sake of performance consistence. Although the highest G' enhancement was obtained from the Stock 2 containing the shortest shell lengths among the given nanoparticles shown in this study, cares must be paid to monitor other tire performances. On the other hand, 20–30% increases in G' were found in Stocks 3 and 4 which contain nanoparticles with moderate shell lengths without increasing their temperature and strain dependences when compared with control Stock 1. Therefore, nanoparticles SBR-PS-2 and SRB-PS-3 with shell M_w over the half of the polymer matrix seem

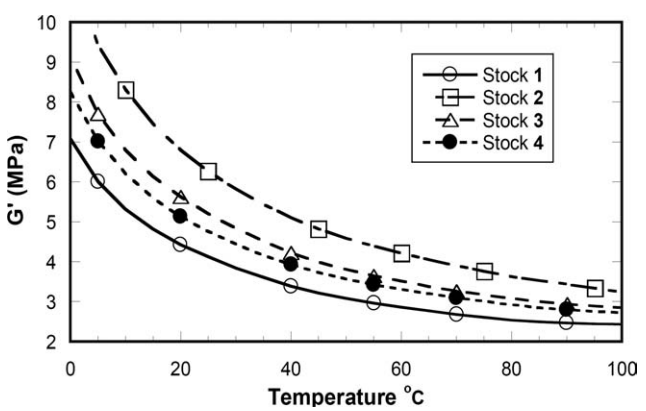

Figure 2 The G' temperature dependences of Stocks 1–4.

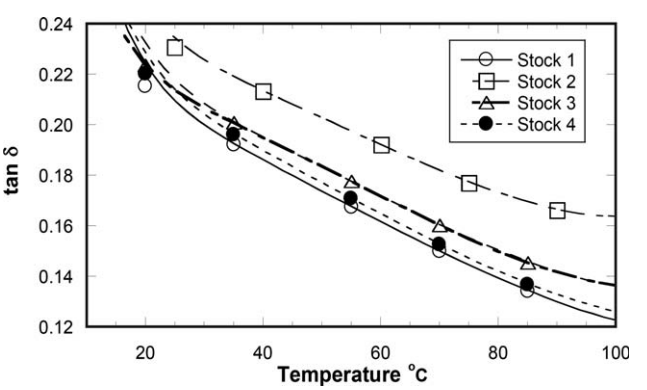

Figure 4 The tan δ temperature dependences of Stocks 1–4.

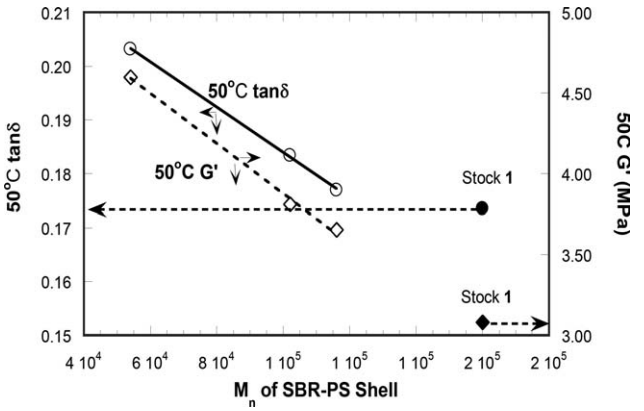

Figure 5 The $G'$and tan δ as a function of the shell molecular weight of the nanoparticle.

ideal to give a tire tread with enhanced and consistent driving handling and cornering performances.

In addition to tire performance consistence concern, compound hysteresis is an another important issue for the compound to be used as tread. Depending upon the tire applications, the desired compound hystereses measured at various temperatures are different.[18] For example, for the racing and high performance tire applications, higher high-temperature (30–100°C) hystereses are required to obtain better road-grip. However, for the general passenger and truck tire applications, reduced rolling resistance is a constant demand from the auto manufactures. This is especially true as the tighter US Corporate Average Fuel Economy (CAFE) standard was imposed on automobile industry.[19] The tire rolling resistance is generally predicted by the compound high-temperature (50–80°C) hysteresis. Therefore, it is desirable to have lower compound high-temperature (50–80°C) hysteresis for the use as the tread to reduce the tire rolling resistance.

The hysteresis temperature dependences of the Stocks 1–4 are shown in Figure 4 where higher hystereses were found in stocks containing nanoparticles with shorter brushes. In contrast, the hysteresis temperature spectrum of Stock 4 is only marginally

TABLE V
Characterization Data of the Polymeric Nanoparticles PBd-PS

	PBd-PS-1	PBd-PS-2
M_w of PBd, g/mole	8780	18,060
M_w of single PS chain in micelle hard core	8.841	9.538
Polydispersity PBd[a]	1.09	1.05
Polydispersity PS[a]	1.12	1.04
% Vinyl[b]	8.4	8.7
Mean Size of Nanoparticle (nm)[c]	8.5	9.8

[a]By GPC measurement.
[b]By 1H-NMR.
[c]By TEM.

higher than those of the Stock 1. Note that there is still a significant improvement in compound G' (20%) for Stock 4 over the control Stock 1. The dependences of compound G' and hysteresis on the shell length of the nanoparticle are summarized in Figure 5. Although Stocks 2 and 3 with shorter brushes enhance the compound G' more effectively, their high-temperature hysteresises also increase when compared to Stock 4. From the hysteresis data of compounds containing nanoparticles with various shell lengths, it seems that the mixing or entanglement and the degree of cocuring between the polymer matrix and nanoparticle may have a strong influence on the resultant compound hysteresis. The shell length of nanoparticles apparently plays an important role on the rubber miscibility and on imparting the compound properties. A study on compatibility between the matrix polymer and the polymeric nanoparticles is thus apparently warranted.

A study on the compatibility between the matrix polymer and the polymeric nanoparticles

To initiate the compatibility study, two polymeric nanoparticles (PBd-PS-1 and PBd-PS-2) with the same styrene-core size (9–10 nm) but contain different PBd-shell brush molecular weight (M_{shell}) of

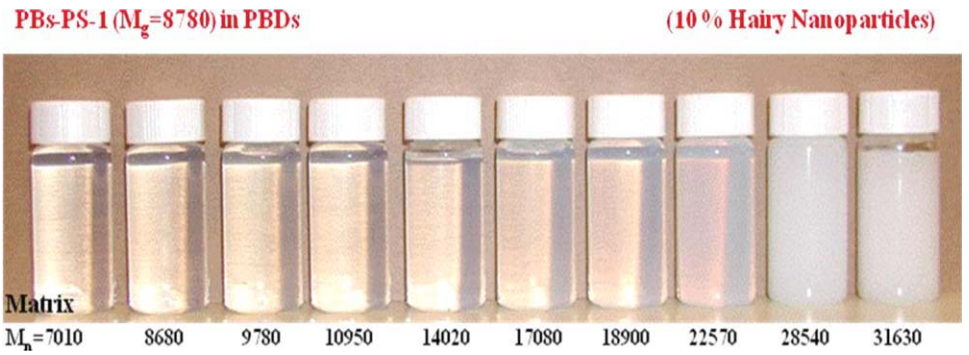

Figure 6 The blend solution of polymeric nanoparticles (PBd-PS) and PBD in hexane. [Color figure can be viewed in the online issue, which is available at wileyonlinelibrary.com.]

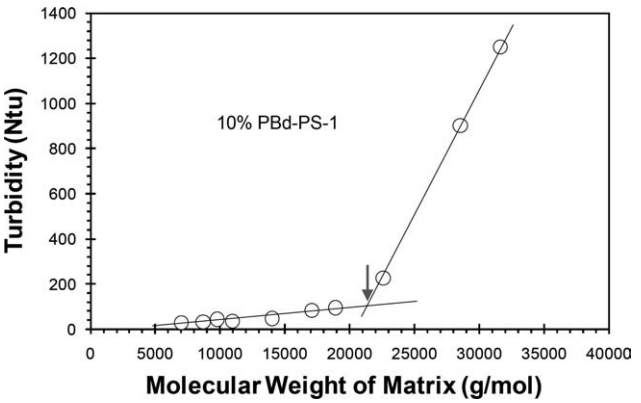

Figure 7 The turbidity (*y*-axis) of the blend (PBd-PS and PBD) solution as a function of the molecular weight of the matrix (PBD).

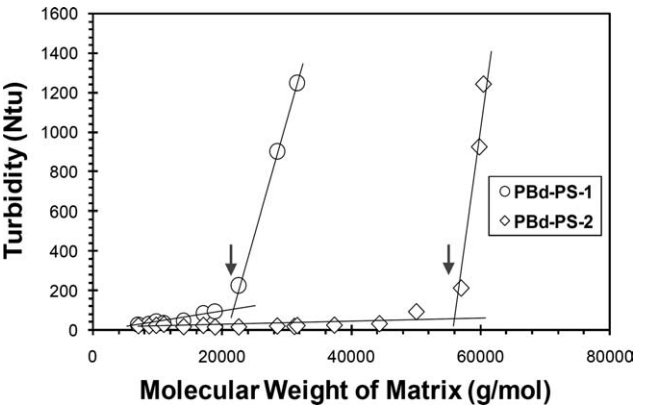

Figure 8 The turbidity (*y*-axis) of the blend (PBd-PS and PBD) solution as a function of the molecular weight of the matrix (PBD).

8,780 and 18,060 g/mole were synthesized. The characterization data of these polymeric nanoparticles are listed in Table V. Ten weight percent of polymeric nanoparticle was then blended into 90 wt % of polybutadienes (PBds) with various molecular weights ranging from M_n= 7,010 to 31,630 g/mole in the hexane solvent. After evaporating the solvent, the phase behaviors of these blends were examined using light scattering. The appearances of these blends shown in Figure 6 were found to be either neatly transparent or completely opaque, depending on the molecular weight of the PBd matrix (M_{matrix}) and M_{shell}. The blend is transparent as M_{matrix} is less than M_{shell}, and it became opaque when M_{matrix} of PBd is greater than 2 M_{shell} of nanoparticle.

The change of interactions between nanoparticle and matrix PBd which lead to the change of the blend phase behaviors can be readily detected by the turbidity measurement. These results are demonstrated in Figure 7 where a sharp transition was found at M_{matrix} of 21,500 g/mole for a given blend composition with a nanoparticle of M_{shell} = 8,780 g/mol. This transition point is the phase separation composition of the blend. For the sake of comparing the blend phase behavior affected by the M_{shell}, a similar methodology was used for blends containing PBd and a nanoparticle with longer M_{shell}. The results are shown in Figure 8 where increased phase transition point was found with increasing M_{shell}. The blend transition occurs at about 21,500 g/mole for nanoparticle with M_{shell} = 8,780, and 55,300 g/mole for that with M_{shell} = 18,060 g/mole. These results suggest that variation of the chain length of the matrix polymer and brush length of the nanoparticle in the blend can change their mutual intimacies. In addition, it also alters the state of aggregation among nanoparticle themselves in the blend. The incompatability between the polymer matrix and nanoparticles may induce additional energy loss upon deformation. Nevertheless, a higher degree of nanoparticle aggregation resulted from the incompatability may induce additional nonlinearity or Payne effect as shown in Figure 9. The mechanical response of the system to oscillating shear is essentially linear in the blend containing low M_w matrix polymer. However, the viscoelastic properties of the blend will strongly depend on applied strain amplitude as it approaches the phase separation point. The increased nonlinearity, in turns, will increase the system hysteresis.[20–24] These results uncovered in the unfilled binary system apparently qualitatively agree with the experimental results shown in the preceeding section of filled rubber compound (See Fig. 5). The agreement suggests an improved reinforcement be obtained in the rubber compound by increasing the degree of compatibility between the polymer matrix and nanoparticles. The fundamentals of dispensing of the brush-type nano-sized particle in the polymer matrix is described in a previous publication.[25]

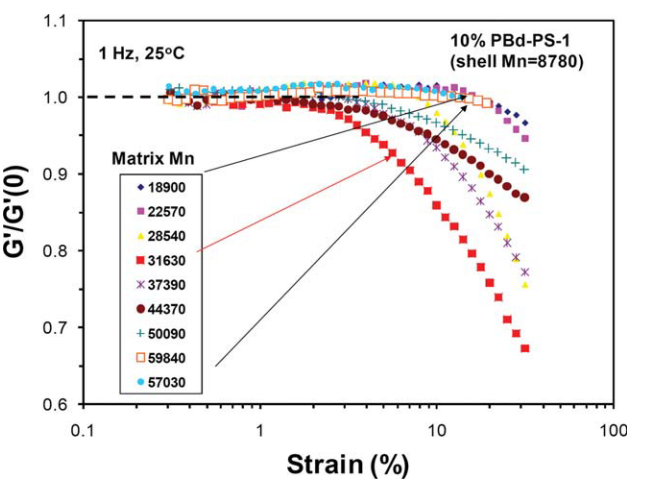

Figure 9 The normalized G' ($G'/G'(0)$)strain dependences of the blend of PBd-PS and PBd as a function of the PBd matrix molecular weight. [Color figure can be viewed in the online issue, which is available at wileyonlinelibrary.com.]

TABLE VI
The Dynamic Viscoelastic Properties Measured by Temperature (TS) and Strain Sweeps (SS) Experiments

Stock No.	tan δ at 0°C (TS)	tan δ at 50°C (TS)	G' at –20°C (TS) (MPa)	$\Delta G'$ MPa 65°C (SS)	tan δ at 5% strain 65°C (SS)
1 control	0.3987	0.1735	53	0.643	0.1297
2	0.3980	0.2032	72.4	1.280	0.1594
3	0.3996	0.1834	63	0.824	0.1365
4	0.3916	0.1769	54	0.700	0.1289

Tire performances predicted by the dynamic viscoelastic properties

The compound dynamic viscoelastic properties used to predict the tire performances are listed in Table VI. The tan δ values measured at different temperatures are usually used to predict several tire performances. For example, tire rolling resistance and wet traction are both dictated by the energy losses from the tire service but encompass different deformation magnitudes and frequencies.[1,2,26,27] These energy losses can be conveniently measured by the dynamic viscoelastic properties of the rubber in a frequency range of 1–10 Hz with strain levels selected as a function of temperature from −100 to 100°C.[18] Thus, use of tan δ at 0°C as a predictor of tire wet traction, tan δ at 50–80°C as a predictor of rolling resistance, and G'at −20°C as a predictor of snow traction are widely practiced in the tire industry.

It is found that Stock 4 which contains the longest brush of the peer SBR-PS nanoparticles listed here, provides the rubber compounds with significant G' enhancement without sacrificing other properties such as snow traction (−20°C G'), wet traction (0°C tan δ), and rolling resistance (50°C tan δ and 65°C tan δ). Therefore, for the passenger and truck tire applications, drive handling and cornering performances can be enhanced without the sacrifice of other performances through the addition of the polymeric nanopartilce with suitable core/shell structure.

Assessing the rubber reinforcement with the addition of nanoparticles—Mechanical properties

The reinforcement of the rubber compounds Stocks 1–4 were further assessed by the tensile mechanical properties and the results are listed in Table VII. Addition of the nanoparticle in the rubber compound improves every tensile mechanical property over the control Stock 1. These improvements include 50% (M50) and 300% Modulus (M300) (8–30%), elongation at break (Eb, 9–17%), tensile strength (Tb,19–31%), and tensile toughness (30–52%). It is also of interest to find that the mechanical strengths and toughness increased in the nanoparticle filled stocks with the increasing shell M_n. A better reinforced rubber compound was obtained through the use of lengthened shell nanoparticles such as SBR-PS-2 and SBR-PS-3. The improved compatibility between the polymer matrix and the hard cores of the nanoparticles were obtained through the lengthened shell which can penetrate, entangle, and cocure into the matrix better. Therefore, increased couplings between the two domains were obtained with reduced interfaces in the nanoparticle filled rubbers. Improved mechanical properties in particle filled rubbers are expected when many of the weak interfaces that were not bounded to the polymer matrix can be eliminated. This seems to be confirmed by the observed improved tensile mechanical properties in the more compatible compound of Stock 4 when compared with Stock 2. The rubber reinforcement by the nanoparticle observed from results of mechanical and dynamic viscoelastic properties are then apparently consistent.

CONCLUSIONS

The reinforcement of the rubber compounds through the use of polymeric nanoparticles was demonstrated. The compound properties including dynamic storage modulus, G', and mechanical properties were improved by the addition of core/shell nanoparticles in rubber compounds. Desirable compound properties can be obtained by adding the nanoparticle with properly tailored structure to eliminate the adverse effect induced by hydrodynamic effect. Addition of nanoparticles with lengthened shell into the compound resulted in obtaining improved mechanical properties with increased G'

TABLE VII
Tensile Mechanical Properties Measured at 25°C

Stock No.	M50 (MPa)	M300 (MPa)	Strength, Tb (MPa)	Elongation at break, Eb (%)	Toughness (MJ/m^3)
1 control	1.59	10.78	15.38	414	30.03
2	1.89	12.20	15.62	374	27.77
3	1.73	11.85	17.40	418	33.53
4	1.70	11.42	18.22	448	37.77

without scarifying other viscoelastic properties such as 0 and 50°C tan δ. The dependences of G' and hysteresis on strain and temperature induced by hydrodynamic effect were also greatly reduced with the use of lengthened shell nanoparticle. In the recognition of the compatibility issue between the polymer matrix and the hard domain of the nanoparticles, the shell size of was demonstrated to have a major impact on the ultimate compound properties described above. The compatibility issue between the host polymer matrix and nanoparticle were studied by examining the phase behaviors of the binary blends with various shell lengths and the molecular weights of the matrix polymer at a given composition. A blend with improved compatibility was obtained with either larger matrix polymer molecular weights or with nanoparticle with lengthened shell size. By using the nanoparticle with lengthened shell for the rubber compounding, it is believed that rubber is reinforced well by eliminating many weak interfaces due to the improved compatibility. Therefore, it is apparent that the shell size in the SBR-PS nanoparticles have to be long enough to entangle or cocure well with the polymer matrix to reduce the high-temperature hysteresis and to enhance the mechanical properties. Favorable and improved tire performances such as cornering, handling, wet traction, snow traction, and rolling resistance can also be attained through the use of the well reinforced rubber by adding properly tailored polymeric nanoparticles.

The authors greatly appreciate the permission of Bridgestone Americas Tire Operations, LLC to publish this work. They also would like to thank the supporting staff of Bridgestone Americas Center for Research and Technology for sample preparation, polymer characterization, and rheological property measurements.

References

1. Futamura, S. Tire Sci Technol 1990, 18, 3.
2. Futamura, S. Rubber Chem Technol 1991, 64, 57.
3. Dunn, J. R. Rubber Chem Technol 1976, 49, 978.
4. Blondel, J. E. Rev Gen Caoutch Plast 1967, 44, 1011.
5. Zelenev, Y. V.; Shvarts, A. G.; Tyurina, V. S.; Nikoforova, A. V.; Zhibaev, V. Y.; Aivazov, A. B. Sov Rubber Technol 1970, 29, 21.
6. Tyurina, V. S.; Shvarts, A. G.; Seidov, N. M.; Eitington, I. I. Sov Rubber Technol 1971, 30, 15.
7. Priklonskaya, N. M.; Tomofeeva, M. J.; Poyarkova, A. D. Sov Rubber Technol 1969, 28, 11.
8. Tyurina, V. S.; Shvarts, A. G.; Eitington, I. I. Sov Rubber Technol 1972, 31, 14.
9. Krom, J.; Wang, X. U.S. Pat. 6,437,050 (2002).
10. Wang, X.; Lin, C.; Hall, J.; Warren, S.; Krom, J.; Kondo, H.; Morita, K. U.S. Pat. 6,956,084 (2005).
11. Wang, X.; Hall, J. E.; Böhm, G. G. A.; Lin, C. J.; James, U.S. Pat. 7,112,369 (2006).
12. Wang, X.; Hall, J. E.; Warren, S.; Krom, J.; Magistrelli, J. M.; Rackaitis, M.; Böhm, G. A. A. Macromolecules 2007, 40, 499.
13. Zhneg, L.; Xie, A. F.; Lean, J. T. Macromolecules 2004, 37, 9945.
14. ASTM Standard D412-98a (2002), Annu. Book ASTM Stand. 2005, 09.01.
15. Einstein, A. Ann Phys 1905, 17, 549.
16. Einstein, A. Ann Phys 1906, 19, 289.
17. Einstein, A. Ann Phys 1911, 34, 591.
18. Wang, M.-J. Rubber Chem Techol 1998, 71, 520.
19. Federal Register, No. 66, Vol. 68, 2003, p. 16867; Department of Transportation, National Highway Traffic Safety Administration, 49 CFR Part 533 [Docket No. 2002-11419; Notice 3] RIN 2127-A170, Light Truck Average Fuel Economy Standards Model Years 2005–2007.
20. Payne, A. R. J Polym Sci 1962, 6, 57.
21. Payne, A. R. J. Appl Polym Sci 1963, 7, 873.
22. Payne, A. R.; Whittaker, R. E. Rubber Chem Technol 1971, 44, 440.
23. Medalia, A. I. Rubber Chem Technol 1978, 51, 437.
24. Kraus, G. J Appl Polym Sci Appl Polym Symp 1984, 39, 75.
25. Wang, X.; Foltz, V. J.; Rackaitis, M.; Böhm, G. A. A. Polymer 2008, 49, 5683.
26. Futamura, S. Rubber Chem Technol 1990, 63, 315.
27. Futamura, S. Rubber Chem Technol 1996, 69, 648.